ARTICLE

OBC
www.rsc.org/obc

Aspergillazines A–E: novel heterocyclic dipeptides from an Australian strain of *Aspergillus unilateralis*

Robert J. Capon,*[a] Ranjala Ratnayake,[a] Michael Stewart,[a] Ernest Lacey,[b] Shaun Tennant[b] and Jennifer H. Gill[b]

[a] *Centre for Molecular Biodiversity, Institute for Molecular Bioscience, The University of Queensland, St. Lucia, Queensland, 4072, Australia. E-mail: r.capon@imb.uq.edu.au; Fax: +61 3 3346 2101; Tel: +61 7 3346 2979*

[b] *Microbial Screening Technologies Pty. Ltd., P.O Box 57, Kemps Creek, New South Wales 2178, Australia*

Received 3rd September 2004, Accepted 28th October 2004
First published as an Advance Article on the web 29th November 2004

Biological and chemical profiling of an Australian strain of the fungus *Aspergillus unilateralis* (MST-F8675), isolated from a soil sample collected near Mount Isa, Queensland, revealed a complex array of metabolites displaying broad chemotherapeutic properties. Noteworthy among these metabolites were a unique series of highly modified dipeptides aspergillazines A–E, incorporating a selection of unprecedented and yet biosynthetically related heterocyclic systems. Co-occurring with the aspergillazines was the recently described marine-derived fungal metabolite trichodermamide A (*cf*. penicillazine), whereas re-fermentation of *A. unilateralis* in NaCl (1%) enriched media resulted in co-production of the only other known example of this structure class, the marine-derived fungal metabolite trichodermamide B. Further investigation of *A. unilateralis* returned the known terrestrial fungal metabolite viridicatumtoxin as the cytotoxic and antibacterial principle, together with *E*-2-decenedioic acid, ferulic acid, (7*E*,7′*E*)-5,5′-diferulic acid and (7*E*,7′*E*)-8,5′-diferulic acid. The aromatic diacids have previously been reported from the chemical and enzymatic (esterase) treatment of plant cell wall material, with their isolation from *A. unilateralis* being their first apparent reported occurrence as natural products. Structures for all metabolites were determined by detailed spectroscopic analysis and, where appropriate, comparison to literature data and/or authentic samples.

Introduction

During our investigations into the chemistry of Australian microbes we have examined the metabolites produced by many Australian terrestrial and marine-derived bacteria and fungi. Recent examples of new fungal metabolites discovered during our studies include aspergillicins A–E from a marine-derived culture of *Aspergillus carneus*[1] and rugulotrosins A–B from a terrestrial *Penicillium* sp.[2] In this report we describe our chemical exploration of an isolate of *A. unilateralis* (MST-F8675) obtained from a soil sample collected near Mount Isa, Queensland, Australia. *A. unilateralis* is not a commonly encountered member of the genus *Aspergillus* and this report represents both the first account of an Australian isolate and the first account of an investigation into the chemistry of *A. unilateralis*. Our interest in *A. unilateralis* was further stimulated by the observation that solvent extracts exhibited both significant antifungal, antibacterial, cytotoxic and nematocidal properties, and displayed an unusual and complex metabolite profile. Our subsequent investigations into *A. unilateralis* revealed viridicatumtoxin (**1**) as the antibacterial and cytotoxic agent. The identity of the antifungal and nematocidal agent(s) has proved more elusive and remains a work in progress. This investigation also yielded a series of known compounds, including *E*-2-decenedioc acid (**2**), ferulic acid (**3**), (7*E*,7′*E*)-5,5′-diferulic acid (**4**), (7*E*,7′*E*)-8,5′-diferulic acid (**5**), riboflavin (**6**) and penicillazine/trichodermamide A (**7**), together with a remarkable series of novel dipeptides, aspergillazines A–E (**8–12**). Re-culture of *A. unilateralis* in NaCl (1%) enriched media led to production of the marine-derived, fungal metabolite trichodermamide B (**13**), suggesting that environmental (*i.e*. media, substrate), rather than genetic factors, influence metabolite expression profiles, at least as they apply to the related analogues **7–13**.

Results and discussion

A solid-phase culture of *A. unilateralis* (MST-F8675) was extracted and fractionated by extensive preparative, semi-preparative and analytical reverse phase chromatography (SPE and HPLC) to yield the known mycotoxin viridicatumtoxin (**1**) as the principle antibacterial and cytotoxic agent. Although first reported in 1973 from *P. viridicatum*,[3] **1** has not featured prominently in subsequent scientific literature. A biosynthetic study in 1982[4] provided comparative spectroscopic data that unambiguously allowed us to confirm the presence of **1** in *A. unilateralis*. Further examination of *A. unilateralis* fractions yielded the recently described novel dipeptide penicillazine (**7**), first reported in 2000 from a marine-derived *Penicillium* sp.[5] Although the original structural proof for **7** was supported by an X-ray analysis, this assignment has since been called into question.[6] In 2003 Fenical *et al.* reported the isolation and identification of trichodermamides A (**7**) and B (**13**) from a marine-derived isolate of *Trichoderma virens*.[6] In assigning complete stereostructures to the trichodermamides, Fenical and coworkers noted that trichodermamide A and penicillazine "…may be identical", implying that the original structure assigned to penicillazine was incorrect. Our re-isolation and assessment of the spectroscopic data (experimental and published) confirms that trichodermamide A and penicillazine are indeed identical and supports the structure assigned by Fenical *et al*.[4]

In addition to identifying viridicatumtoxin (**1**) and the novel marine-derived, fungal metabolite penicillazine/trichodermamide A (**7**), the *A. unilateralis* extract yielded trace amounts (~700 μg) of a new penicillazine analogue with a MW 16 amu higher than penicillazine (**7**). While such an analogue might easily be dismissed as a mildly interesting minor oxidized co-metabolite (or artefact), these conclusions were inconsistent

DOI: 10.1039/b413440k

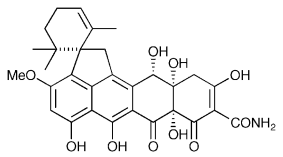

(**1**)

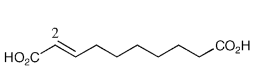

(**2**)

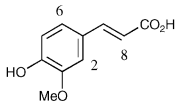

(**3**)

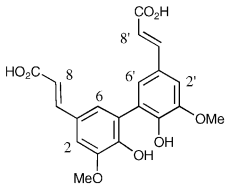

(**4**)

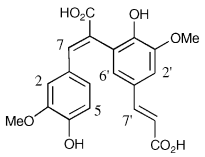

(**5**)

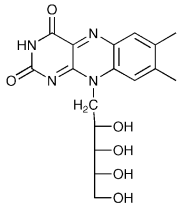

(**6**)

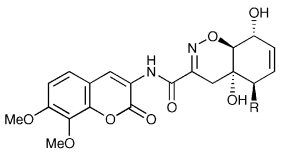

(**7**) R = OH penicillazine/trichodermamide A
(**13**) R = Cl trichodermamide B

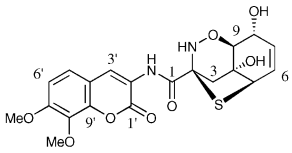

(**8**) aspergillazine A

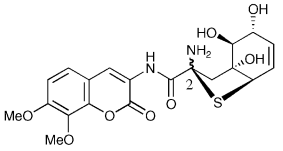

(**9**) and (**10**) C-2 epimers
aspergillazines B and C

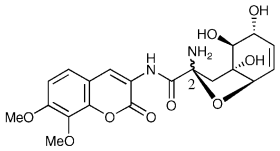

(**11**) and (**12**) C-2 epimers
aspergillazines D and E

with accurate mass measurements that revealed a molecular composition for an analogue of **7** in which an oxygen atom was replaced by sulfur. As the full extent of knowledge about the penicillazine/trichodermamide structure class is based on only two compounds, **7** and **13**, both of which have come to light in the last few years and neither of which incorporate sulfur, the detection of sulfur analogues was noteworthy. Lacking sufficient material for a full spectroscopic characterization and structure assignment, we re-fermented *A. unilateralis* under optimised conditions while monitoring metabolite production by HPLC (DAD and ELSD).

Fractionation of the second *A. unilateralis* fermentation optimised for the production of penicillazine/trichodermamides once again yielded **1** and **7**, but also resulted in increased production of a suite of metabolites barely detected in the first culture. These metabolites were loosely fractionated into materials that were deemed "penicillazine like", as well as those that were deemed "not penicillazine like".

Further purification of the latter fractions yielded a selection of metabolites including the known fungal metabolite *E*-2-decenedioic acid (**2**),[7] as well as ferulic acid (**3**), (7*E*,7′*E*)-5,5′-diferulic acid (**4**),[8] (7*E*,7′*E*)-8,5′-diferulic acid (**5**)[8] and riboflavin (**6**). The structures assigned to **3** and **6** were confirmed by comparison to authentic commercial samples, whereas **2**,[7] **4**[8] and **5**[8] were confirmed by spectroscopic comparison to literature data.

Of this set of metabolites, *E*-2-decenedioic acid (**2**) was particularly noteworthy in so far as it had previously been reported as a weak nematocidal agent isolated from the wood rotting fungus *Pleurotus ostreatus*. In those earlier studies it had been proposed that **2** played an integral role in the *P. ostreatus* predation strategy by inducing a paralysis in free living nematodes prior to mycelial invasion and digestion.[7] While in our hands, extracts of *A. unilateralis* were observed to display a characteristic paralytic activity against the commercial livestock parasite *Haemonchus contortus* and we can confirm that *E*-2-decenedioic acid (**2**) was not active against *H. contortus*. The identity of the nematocidal agent in *A. unilateralis* remains a work in progress.

With respect to **3–5**, whereas ferulic acid (**3**) is a known plant metabolite,[9] the only reported "natural" occurrence of the two isomeric dimers (7*E*,7′*E*)-5,5′-diferulic acid (**4**) and (7*E*,7′*E*)-8,5′-diferulic acid (**5**) has been from the chemical and enzymatic (esterase) treatment of plant cell wall material.[8,10,11] Thus, the isolation of **4** and **5** from *A. unilateralis* would appear to represent their first reported occurrence as natural products. Biosynthetically, **4** and **5** are oxidative dehydrodimers of **3**. All three are known to bind *via* ester linkages to plant cell walls with the *in situ* formation of ferulic dimers such as **4** and **5** leading to cross-linking between polysaccharide and/or lignan strands.[8,10] Cross-linking has a marked influence on cell wall properties, and hence the structural characteristics of plants, through enhancing structural integrity and inhibiting degradation. Reported mechanisms for dimerization include photochemically induced [2 + 2]-cyclodimerization and oxidative coupling *via* the action of peroxidases.[8] The recovery of **3–5** in this study may be indicative of the *de novo* biosynthetic capability of *A. unilateralis* or, alternatively, may reflect the capacity of *A. unilateralis* to deploy esterases to process media constituents (*i.e.* wheat).

Fractionation of *A. unilateralis* also yielded a series of penicillazine like metabolites, of which aspergillazine A (**8**) proved to be the minor sulfur containing metabolite encountered in the earlier culture (see above). Moreover, aspergillazines B (**9**) and C (**10**) were isomeric reduced analogues also bearing sulfur, whereas aspergillazines D (**11**) and E (**12**) were oxygen analogues

Table 1 NMR (CD_3OD, 400 MHz) data for aspergillazine A (**8**) and the minor *cis* amide conformational isomer **8a**

No.	^{13}C (**8**) (ppm)[a]	^{1}H (**8**) δ (m, J/Hz)	DQFCOSY (**8**)	gHMBC (**8**)	^{1}H (**8a**) δ (m, J/Hz)
1′	158.1				
2′	121.4				
3′	118.4	6.96 (s)		C-1′, C-5′, C-9′	6.74 (s)
4′	115.3				
5′	129.3	7.03 (d, 9.0)	H-6′	C-3′, C-7′, C-9′	7.86 (d, 8.8)
6′	105.8	6.63 (d, 9.0)	H-5′	C-4′, C-8′	6.46 (d, 8.8)
7′	156.0				
8′	138.0				
9′	149.0				
7′-*OMe*	56.4	3.87 (s)		C-7′	3.84 (s)
8′-*OMe*	61.1	3.80 (s)		C-8′	3.77 (s)
1	162.1				
2	77.2				
3_a	50.9	3.11 (d, 11.7)	H-3_b	C-1, C-2, C-4, C-5, C-9	[b]
3_b		2.38 (d, 11.7)	H-3_a	C-2, C-4, C-5, C-9	[b]
4	76.1				
5	47.7	4.13 (bd, 5.1)	H-6	C-4, C-6, C-7	4.11 (d, 5.3)
6	126.1	5.92 (ddd, 10.0, 5.1, 1.0)	H-5, H-7	C-4, C-5, C-8	[b]
7	128.4	6.05 (ddd, 10.0, 4.8, 1.1)	H-6, H-8	C-8, C-9	[b]
8	65.3	4.33 (bd, 4.8)	H-7	C-4, C-6, C-7, C-9	4.29 (m)
9	81.9	4.19 (m)		C-5, C-7, C-8	4.15 (m)

[a] ^{13}C NMR assignments are supported by a DEPT experiment. [b] Resonances overlap those for **8**.

that re-equilibrated to a 1 : 0.85 mixture on standing. The structure elucidation of aspergillazines A–E (**8–12**) is outlined below.

High resolution ESI(+)MS analysis of aspergillazine A (**8**) returned a pseudo molecular [M + Na] ion consistent with a molecular formula ($C_{20}H_{20}N_2O_8S$, Δ = +0.6 mmu) requiring 12 double-bond equivalents. Comparison of the NMR data for aspergillazine A (**8**) with that for **7** confirmed a common dimethoxyaminocoumarin *N*-terminus and a closely related *C*-terminus. More specifically, analysis of the ^{1}H NMR data for the *N*-terminus (C-1′ to C-9′) in **8** (see Table 1) revealed characteristic *ortho* coupled aromatic methines (δ_H 7.03 and 6.63, J = 9.0 Hz), two aromatic OMe substituents (δ_H 3.87 and 3.80) and an H-3′ methine (δ_H 6.96). The last resonance is noteworthy for being significantly shielded (Δ_δ 1.64) relative to the same proton in **7** (δ_H 8.59); a fortuitous effect that will be addressed later in this report. This deviation in the chemical shift of H-3′ notwithstanding, the ^{13}C, DQFCOSY, gHMQC and gHMBC NMR data for **8** (see Table 1) were fully consistent with the *N*-terminus as indicated, with gHMBC correlations from H-3′ to C-5′ and from the 7′ and 8′ OMe to C-7′ and C-8′ respectively, confirming the substitution pattern as shown. Comparable analysis of the ^{1}H NMR data for the *C*-terminus (C-1 to C-9) in **8** (see Table 1) revealed two isolated spin-systems. The first consisted of a sequence from H-5 through to H-9, while the second was an isolated diastereotopic methylene (H-3_a and H-3_b). That H-6 and H-7 were olefinic methines, and H-8 and H-9 were oxymethines, was apparent from the respective ^{13}C NMR shifts for C-6 (δ_C 126.1), C-7 (δ_C 128.4), C-8 (δ_C 65.3) and C-9 (δ_C 81.9). The *cis* configuration between H-6 and H-7 was apparent from a diagnostic $J_{6,7}$ (10.0 Hz). The deshielded H-5 resonance in **8** was attributed to a thiomethine based both on the ^{13}C NMR shift for C-5 (δ_C 47.7) and the limited options for incorporation of a sulfur atom into the *C*-termini of **8**. By comparison, the corresponding ^{13}C NMR shifts for the hydroxylated C-5 in **7** were reported as δ_C 73.0 (d_6-DMSO)[6] and δ_C 75.2 ($CDCl_3$),[5] while for the chlorinated analogue **13** C-5 resonates at δ_C 65.8 (d_6-DMSO).[6]

Key gHMBC correlations in **8** (see Table 1), from H-5 to C-4 and from H-8 to C-4, supported closure of the six-membered ring through an oxygenated C-4 quaternary carbon (δ_C 76.1). Similarly, gHMBC correlations from H-3_a and H-3_b to C-4 and C-5 positioned the isolated diastereotopic methylene spin-system as indicated. The remaining quaternary carbon flanking H-3_a and H-3_b was readily identified by gHMBC correlations as C-2 (δ_C 77.2), with a further correlation from H-3_a to C-1 (δ_C 162.1) positioning the amide carbonyl of the *C*-termini. With one of two nitrogen atoms in **8** accommodated by the amide linkage, the remaining nitrogen atom must be substituted at C-2 (as for **7**). It is interesting to note that whereas the ^{13}C NMR (CD_3OD) resonance for C-2 in **7** (δ_C 151.4, s) indicated an oximino sp^2 hybridized carbon, the corresponding resonance for C-2 in **8** (δ_C 77.2, s) revealed a quaternary sp^3 hybridized carbon. In order to accommodate all of these observations, **8** can be viewed as a cyclized analogue of **7** in which an additional heterocyclic ring has assembled through intramolecular nucleophilic addition at C-2. That this process retains the N–O heteroatom linkage from C-2 to C-9 is evidenced by excellent ^{1}H NMR (CD_3OD) comparison between H-9 in **7** (δ_H 4.19) *versus* **8** (δ_H 4.19), as compared to aspergillazines B–E (**9–12**) (δ_H 3.68–3.71) where this N–O heterocycle has been cleaved (see Table 2). Given this analysis, formation of the new heterocycle is more likely through a C-2 to C-5 thiophane linkage, as indicated, than the alternative C-2 to C-4 oxetane linkage, inferred from spectroscopic, thermodynamic and biosynthetic considerations. Following this reasoning, the putative biosynthetic precursor to aspergillazine A (**8**) would be a C-5 thiol analogue of **7**. Fig. 1 displays a representation of the *C*-termini for penicillazine (**7**), aspergillazine A (**8**) and the proposed thiol precursor to **8**. This analysis clearly reveals the favourable proximity of the C-5 thiol substituent and the C-2 oximino carbon, as well as the relative ease with which the intramolecular nucleophilic addition of the C-5 thiol to the C-2 oximino system could take place.

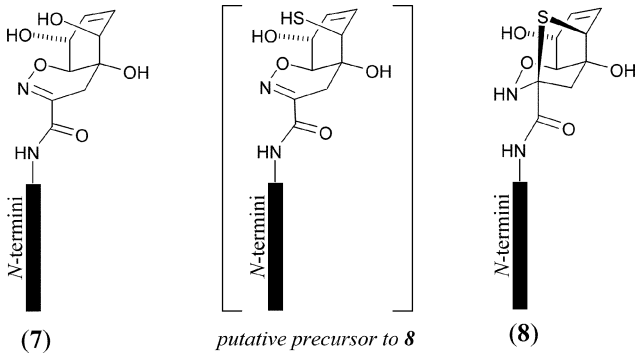

Fig. 1 Representation of penicillazine (**7**), aspergillazine A (**8**) and the proposed biosynthetic precursor to **8**.

Table 2 ^{1}H NMR (CD_3OD, 600 MHz) data for aspergillazines B–E (**9–12**) and selected resonances for minor *cis* amide conformational isomers **9a–12a**

	^{1}H δ (m, J/Hz)[a]			
No.	**9**	**9a**	**10**	**10a**
3′	6.93 (s)	6.75 (s)	6.90 (s)	7.72 (s)
5′	7.07 (d, 8.5)	7.40 (d, 8.9)	7.06 (d, 8.8)	7.41 (d, 9.0)
6′	6.64 (d, 8.5)	6.43 (d, 8.9)	6.63 (d, 8.8)	6.47 (d, 9.0)
7′-*OMe*	3.88 (s)	3.84 (s)	3.87 (s)	3.85 (s)
8′-*OMe*	3.82 (s)	3.82 (s)	3.80 (s)	3.78 (s)
3_a	2.85 (d, 15.0)	2.79 (dd, 14.8, 1.0)	2.90 (d, 13.9)	2.89 (d, 13.9)
3_b	2.51 (d, 15.0)	2.49 (d, 14.8)	2.37 (dd, 13.9, 1.0)	2.33 (dd, 13.9, 1.0)
5	4.04 (m)	[b]	4.25 (m)	[b]
6	5.53 (ddd, 10.0, 2.0, 2.0)	[b]	5.47 (m)	[b]
7	5.64 (ddd, 10.0, 2.0, 2.0)	[b]	5.47 (m)	[b]
8	4.15 (ddd, 8.0, 2.5, 2.0)	4.21 (m)	4.11 (dd, 8.4, 3.2)	[b]
9	3.69 (d, 8.0)	[b]	3.70 (d, 8.4)	3.69 (d, 8.2)
	11	**11a**	**12**	**12a**
3′	6.91 (s)		6.94 (s)	
5′	7.05 (d, 8.8)		7.06 (d, 8.8)	
6′	6.63 (d, 8.8)		6.64 (d, 8.8)	
7′-*OMe*	3.88 (s)	3.86 (s)	3.88 (s)	3.86 (s)
8′-*OMe*	3.80 (s)	3.79 (s)	3.80 (s)	3.79 (s)
3_a	2.91 (d, 14.0)	2.89 (d, 14.0)	2.69 (d, 15.0)	2.67 (d, 15.0)
3_b	2.11 (d, 14.0)	2.08 (d, 14.0)	2.38 (d, 15.0)	2.38 (d, 15.0)
5	4.25 (m)	[b]	4.45 (m)	[b]
6	5.47 (ddd, 10.2, 2.5, 2.3)	[b]	5.62 (ddd, 10.2, 2.5, 2.3)	[b]
7	5.59 (ddd, 10.2, 1.6, 1.4)	[b]	5.69 (ddd, 10.2, 1.5, 1.4)	[b]
8	4.11 (dd, 8.0, 3.2)	[b]	4.14 (ddd, 8.4, 2.1)	[b]
9	3.68 (d, 8.0)	[b]	3.71 (d, 8.4)	[b]

[a] The equilibrium ratio of *trans* to *cis* conformational isomers (**9, 9a, 10a, 11a** and **12a**) is 1 : 0.2. The equilibrium ratio of C-2 epimers (**11 : 12** and **11a : 12a**) is 1 : 0.85. [b] Resonances overlap those for *trans* isomers.

At this point it is useful to draw attention to a minor "inseparable isomer" **8a** that persisted at a constant **8** : **8a** ratio of 1 : 0.2 in all chromatographic fractions and samples of **8**, as demonstrated in the ^{1}H NMR data (see Table 1). Variable temperature ^{1}H NMR (d_5-pyridine) data confirmed an equilibrium relationship, with the resonances attributed to **8** and **8a** shifting through intermediate chemical shifts and/or coalescing at elevated temperatures. Two possible explanations for this equilibrium are as follows; (a) **8a** is the putative thiol biosynthetic precursor mentioned above (and displayed in Fig. 2), or (b) **8a** is an alternative conformational isomer about the amide bond. We discount explanation (a) on the grounds that the ^{1}H NMR shift for H-3′ is significantly deshielded in co-metabolite **7** which possesses a C-2 oximino functionality as detailed above. This deshielding influence is presumably a function of extended conjugation from the aromatic system of the aminocoumarin through the amide to the oximino functionality in **7**, and/or a preferred conformation that exposes H-3′ to the deshielding influence of the amide carbonyl. In either event, given that H-3′ resonates at a higher field for both **8** (δ_H 6.96) and **8a** (δ_H 6.74), this would mitigate against the minor isomer possessing an oximino C-2. The ^{1}H NMR data is however consistent with **8** and **8a** being alternative conformational isomers about the amide bond linking the *N*- and *C*-termini. That such isomers are evident for **8**/**8a** but not **7** is possibly a function of extended conjugation and/or co-planarity imposed across C-1 to C-3, incorporating the amide nitrogen and oximino heterocycle atoms in **7** compared to **8**/**8a**. Fig. 2 illustrates possible penicillazine *trans* (**7**) and *cis* (**7a**) amide conformational isomers and suggests a higher degree of steric interaction with the *N*-termini in the *cis versus* the *trans* form.

Free rotation about the C-1 to C-2 bond in **7** is impeded both by the co-planar requirements for conjugation and the need to retain an *anti* relationship between the C=O and C=N dipoles. It is proposed that unfavourable steric interactions ensure that **7** exists overwhelmingly as the *trans* amide conformational isomer. By contrast, comparable analysis for aspergillazine A (**8**) (see Fig. 2) indicate that, without the imposition of extended conjugation and associated co-planarity across the amide and oximino functionalities, the higher energy *cis* amide conformational isomer possesses additional C-1 to C-2 rotational freedom that could alleviate steric stress. This hypothesis could explain the

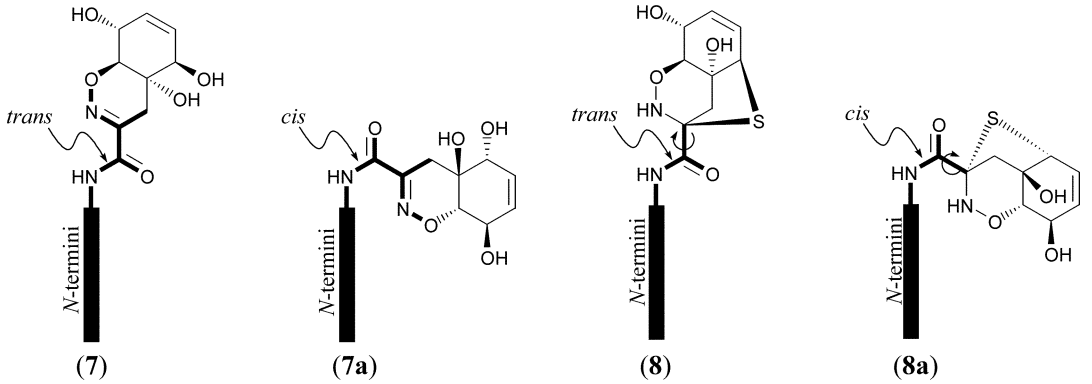

Fig. 2 Representation of penicillazine *trans* (**7**) and *cis* (**7a**), and aspergillazine A *trans* (**8**) and *cis* (**8a**) amide conformational isomers, highlighting co-planar atoms in the *C*-termini and additional rotational freedom in **8**/**8a** compared to **7**/**7a**.

co-occurrence of major *trans* (**8**) and minor *cis* (**8a**) amide conformational isomers.

The proposed structure for aspergillazine A (**8**) requires a fixed relative stereochemistry about C-2, C-4, C-5 and C-9, whilst modelling of the H-7 to H-8 dihedral angle (Chem3D) for α and β C-8 hydroxy epimers favours a C-8 α hydroxy substituent (exp $J_{7,8} = 4.8$ Hz). Given that **8** co-occurs with **7** and possesses a common relative stereochemistry, on biosynthetic grounds we propose a common absolute stereochemistry.[6]

High resolution ESI(+)MS analysis of the minor co-metabolites aspergillazines B (**9**) and C (**10**) returned pseudo molecular [M + Na] ions consistent with an isomeric molecular formula ($C_{20}H_{22}N_2O_8S$, $\Delta = -0.6$ and -0.1 mmu respectively) requiring one less double bond equivalent than that for aspergillazine A (**8**). Sharing a common *N*-terminus with **7** and **8**, as evidenced by ^{1}H NMR data (see Table 2), both **9** and **10** also possess a closely related *C*-terminus complete with amide linkage and a $\Delta^{6,7}$ functionality. These observations require that **9** and **10** are ring-opened analogues of **8**. Individually displaying both major *trans* and minor *cis* amide conformational isomers (1 : 0.2), both with diagnostic shielded ^{1}H NMR resonances for H-3′ (see Table 2), suggests that **9** and **10** possess an sp^3 hybridized C-2, common with that in **8**. Both **9** and **10** possess very similar ^{1}H NMR data (see Table 2) which, on comparison to **8**, display shift differences associated with H-3_a, H-3_b and H-9, consistent with reduction and ring opening of the 1,2-oxazine as indicated. Particularly noteworthy is the Δ_δ 0.5 upfield shift associated with H-9 on conversion from the 1,2-oxazine (**8**) to the acyclic variant (**9** and **10**). In this analysis, **9** and **10** are proposed to be C-2 epimers derived from **8** *via* reductive ring opening of the 1,2-oxazine. Prolonged storage of **9** and **10**, including lengthy exposure to NMR data acquisition at room temperature, revealed no hint of equilibration. Thus, somewhat surprisingly, the unique C-2 amino thiophane functionality in **9** and **10** does not display typical *acetal* properties of equilibration through an acyclic *imine* intermediate.

High resolution ESI(+)MS analysis of the remaining minor co-metabolites, an equilibrating mixture of aspergillazines D (**11**) and E (**12**), returned a pseudo molecular [M + Na] ion consistent with a molecular formula ($C_{20}H_{22}N_2O_9$, $\Delta = +0.7$ mmu) equivalent to **9** and **10**, in which the sulfur atom has been replaced by oxygen. Following a structural argument comparable to that outlined above for **9** and **10**, aspergillazines D (**11**) and E (**12**) can be identified as C-2 epimeric structures incorporating the C-2 amino tetrahydrofuran functionality as shown. Unlike **9** and **10**, following separation by HPLC the epimers **11** and **12** underwent rapid equilibration to a 1 : 0.85 mixture. Thus, the unique C-2 amino tetrahydrofuran functionality in **11** and **12** does display typical *acetal* properties of equilibration through an acyclic *imine* intermediate, presumably as illustrated in Fig. 3.

It is satisfying to note a common equilibrium dynamic across the natural products described above. Whereas all the C-5 thiol analogues **8**, **9** and **10** display irreversible nucleophilic addition to a C-2 oximino/imino precursor, the corresponding C-5 hydroxy analogues **7**, **11** and **12** either show no nucleophilic addition (*i.e.* **7**) or, having undergone addition, engage in rapid equilibrium through an imino intermediate (*i.e.* **11** and **12**). These observations either point to a remarkably C-2 selective reactivity when confronted with sulfur *versus* oxygen nucleophiles, or highlight differences in ring-strain between the differing heterocyclic systems.

The relative and absolute stereochemistry of **9–12** are tentatively assigned as shown on the basis of ^{1}H NMR comparisons to aspergillazine A (**8**) and on biogenetic grounds by comparison to the co-metabolite penicillazine (**7**). The aspergillazines A–E (**8–12**) possess unique heterocyclic systems and offer unique insights into the relative reactivity and stability of these heterocycles. These systems are the subject of ongoing synthetic investigations with the view to gaining access to new chemical space and exploring both the fundamental chemistry and possible biological applications of these novel systems.

While our re-fermentation of *A. unilateralis* was optimised for the production of aspergillazines, we are aware that the highly antifungal (against *S. cerevisiae*) and nematocidal agents detected in the first culture remain unidentified. Clearly the biomolecular potential of *A. unilateralis* has yet to be exhausted and is deserving of ongoing attention.

Experimental

General procedures

High-performance liquid chromatography (HPLC) was performed using a Waters 2790 Separations Module equipped with a Waters 996 Photodiode Array Detector, Alltech 500

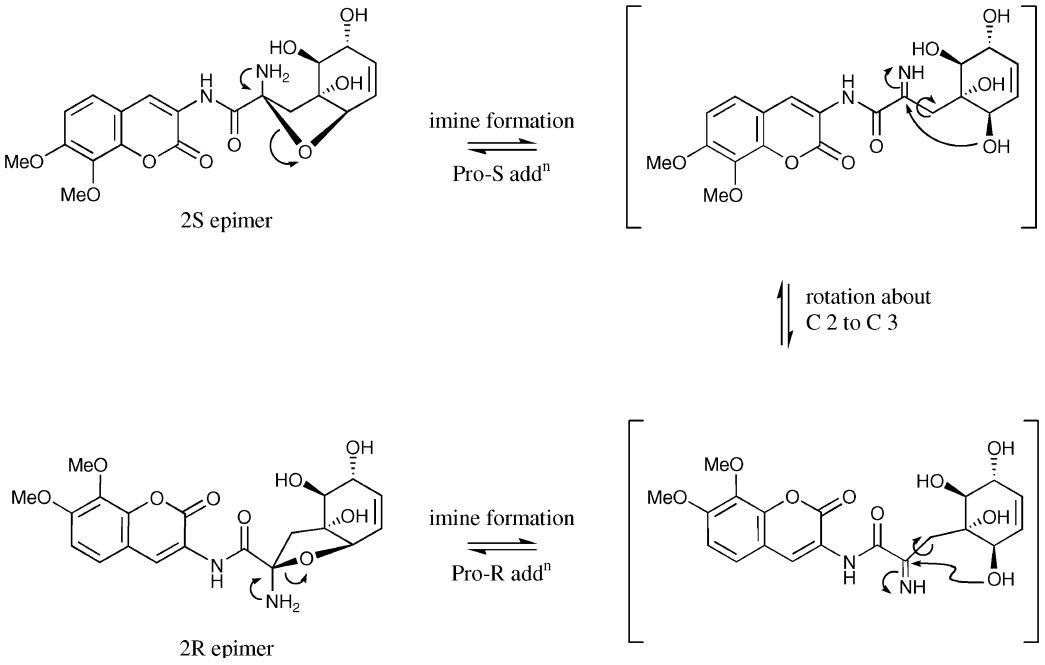

Fig. 3 Proposed mechanism for C-2 epimer equilibration between aspergillazine D (**11**) and aspergillazine E (**12**).

Evaporative Light Scattering Detector and a Waters Fraction Collector II, operating under Waters Millennium software or an Agilent 1100 Series Separations Module, Agilent 1100 Series Diode Array and/or Multiple Wavelength Detectors, Polymer Laboratories PL-ELS1000 Evaporative Light Scattering Detector (ELSD) and Agilent 1100 Series Fraction Collector and running ChemStation Rev.9.03A and Purify version A.1.2 software. ^{1}H and ^{13}C NMR spectra were performed on one or more of Varian Inova 400, Varian Unity 400 plus, Bruker Avance 500 or Bruker Avance 600 spectrometers, in the solvents indicated (referenced to residual ^{1}H signals in the deuterated solvents, and J values in Hz). ESI(±)MS were acquired using a Micromass ZMD mass detector or an Agilent 1100 series LC/MSD. High resolution (HR) ESI-MS measurements were obtained on a Finnigan MAT 900 XL-Trap instrument with a Finnigan API III source. Chiroptical measurements ($[\alpha]_D$) were obtained on a Jasco P-1010 Intelligent Remote Module type polarimeter in a 100 by 2 mm cell (units 10^{-1} deg cm^2 g^{-1}), while Ultraviolet (UV) absorption spectra were obtained using a CARY3 UV visible Spectrophotometer. IR spectroscopic data were not obtained due to insufficient material, solubility issues and the need to subject the available samples to different bioassays.

Bioassay

Cytotoxic activity was determined in a microtitre plate, cell proliferation assay. Murine NS-1 cells in RPMI 1640 medium (200 μL, 5×10^4 cells mL^{-1}), supplemented with 1 mM sodium pyruvate and 5% (v/v) newborn calf serum, were added to the wells of a microtitre plate containing serial two-fold dilutions of the test compound. The plates were incubated at 37 °C in the presence of 5% CO_2. A qualitative assessment of cell proliferation was made at 72 h, with the LD_{99} determined as the lowest concentration of the test compound at which no cell proliferation was observed.

Antibacterial activity was determined in an agar-based, microtitre plate assay. An aliquot of an overnight fermentation of *Bacillus subtilis* (ATCC 6633) was applied to the surface of an agar matrix that contained the test compound, which was then incubated at 28 °C. A qualitative assessment of bacterial growth was made at 24 h, with the MIC determined as the lowest concentration of the test compound at which no growth of bacteria was observed.

Antifungal activity was determined in an agar-based, microtitre plate assay. An aliquot of an overnight fermentation of *Saccharomyces cerevisiae* (ATCC 9763) or *Candida albicans* (ATCC 10231) was applied to the surface of an agar matrix containing the test compound, which was then incubated at 28 °C. A qualitative assessment of yeast growth was made at 24 h, with the MIC determined as the lowest concentration of the test compound at which no growth of yeast was observed.

Nematocidal activity was determined by the method of Gill *et al.*[12] in which *Haemonchus contortus* eggs were applied to the surface of an agar matrix containing the test sample and supplemented with a nutrient medium. The eggs were allowed to hatch and develop through to the L3 infective stage. A qualitative assessment of the larvae was made on day 6 of the assay to determine the lowest concentration of the test compound at which 99% of the larvae present were affected.

Collection and fungal isolation

The fungus *A. unilateralis* (MST-F8675) was isolated on malt extract agar from a soil sample collected 24 km west of Mount Isa, Queensland, Australia.

Fermentation and metabolite isolation

Fermentation 1. Initial investigation of the metabolic capabilities of *A. unilateralis* focused on production at 22 °C or 28 °C for 21 days on malt extract agar (5 × 15 g) or wheat (50 g). The agar and mycelia for each culture were extracted with MeOH (2 mL per g of solid) for 24 h at 28 °C, decanted and a portion concentrated *in vacuo* and tested for a broad range of biological activities. These assays revealed antifungal activity against *Saccharomyces cerevisiae*, cytotoxicity against NS-1 cells, antibacterial activity against *Bacillus subtilis* and nematocidal activity against *H. contortus*. The latter activity was of note in that it was characterized by an uncommon paralytic effect. HPLC analysis (PDA) of the extracts revealed a relatively low level production of secondary metabolites, some of which possessed UV spectra not previously encountered in the genus *Aspergillus*. Metabolite production was maximal when the fungus was cultured on wheat.

The MeOH extracts from the first scaled up cultures were pooled (~200 mL), diluted with H_2O (600 mL), and, after adjusting to pH 7, the resulting suspension was adsorbed onto 2 × 10 g C_{18} Bond Elute SPE cartridges. Elution with H_2O removed the polar metabolites, while subsequent elution with MeOH (80 mL) recovered non-polar neutral and basic metabolites. The pH of the aqueous eluent was subsequently adjusted to 4 and the suspension re-adsorbed onto the same two C_{18} Bond Elute SPE cartridges. Elution with MeOH returned non-polar acidic metabolites.

The combined MeOH eluents (non-polar metabolites) were concentrated *in vacuo* (441 mg) and solvent partitioned between *n*-BuOH (100 mL) and H_2O (100 mL). The *n*-BuOH soluble material (244 mg) was concentrated *in vacuo* and further partitioned between 20% H_2O–MeOH (100 mL) and petroleum spirit (100 mL). The aqueous MeOH soluble material was then diluted with H_2O (60 mL) and further partitioned against CH_2Cl_2 (160 mL). The biologically active CH_2Cl_2 solubles (*S. cerevisiae* LD_{99} 21 μg mL^{-1}) were concentrated *in vacuo* (64.6 mg) and further fractionated by elution through a C_{18} SPE cartridge (2 g, Alltech, 5% stepwise gradient from 50% H_2O (0.05% TFA)–MeOH, to MeOH). The fraction eluting in 45% H_2O (0.05% TFA)–MeOH (13.7 mg) did not inhibit *S. cerevisiae* but did display interesting ^{1}H NMR resonances, whereas the fraction eluting with 20% H_2O (0.05% TFA)–MeOH (16.5 mg) displayed potent antifungal activity against *S. cerevisiae* (LD_{99} 2.8 μg mL^{-1}). The former fraction was further purified by C_{18} HPLC column (2.5 mL min^{-1} gradient from 75% H_2O (0.05% TFA)–MeCN to 60% H_2O (0.05% TFA)–MeCN over 20 minutes through a Zorbax-RX C_8 5 μm 250 × 9.4 mm column) to yield penicillazine A (**7**) (1.5 mg, 0.34% yield) and trace amounts of aspergillazine A (**8**) (0.7 mg, 0.16% yield). The latter bioactive fraction was further purified by C_{18} HPLC (2.5 mL min^{-1} isocratic 35% H_2O–MeCN through a Zorbax-RX C_8 5 μm 250 × 9.4 mm column) to yield viridicatumtoxin (**1**) (2.8 mg, 0.63% yield), with modest activity against *C. albicans* (LD_{99} 25 μg mL^{-1}) and more significant cytotoxicity (LD_{99} 0.78 μg mL^{-1}) and activity against *B. subtilis* (LD_{99} 13 μg mL^{-1}). All yields are calculated relative to the dry weight of the combined MeOH eluants (441 mg) prior to HPLC.

Fermentation 2. The pooled MeOH extracts (2.75 L) from a second scaled up solid phase fermentation of *A. unilateralis* (MST-F8675) (20 × ~30 g wheat, 21 days, 28 °C) were diluted with H_2O to 8 L and the pH adjusted to 9 through the addition of Et_3N. This suspension was then eluted in 2 L parallel aliquots through 4 × 10 g Varian HF C_{18} SPE cartridges, followed by sequential elution with 50% H_2O–MeOH (40 mL) then MeOH (40 mL). The pH of the initial aqueous eluant was adjusted to 4 by the addition of TFA and re-eluted through the same C_{18} SPE cartridges, followed by a similar sequential elution to afford 50% H_2O–MeOH (40 mL) then MeOH (40 mL) fractions. The combined 50% H_2O–MeOH eluants were concentrated *in vacuo* (671 mg) and subjected to preparative HPLC (single injection, 60 mL min^{-1}, gradient elution of 90–60% H_2O (0.01% TFA)–MeCN over 20 min followed by MeCN (0.01% TFA) for 10 min,

through a Platinum EPS C_{18} 5 μm 50 × 100 mm column). The eighty fractions acquired from preparative HPLC were pooled to 30 fractions based on analytical HPLC and flow injection ESI(±)MS analysis.

Those fractions containing "penicillazine like" metabolites were identified by a combination of UV, ESI(±)MS and ^{1}H NMR spectroscopy and were subjected to multiple serial fractionation by HPLC (2.0–2.5 mL min^{-1} gradient elution from 80–75% H_2O–MeCN to 50% H_2O–MeCN over 20–30 min through a Phenomenex LUNA C_8 5 μm (2) 250 × 10 mm column and/or by comparable elution through a Zorbax-RX C_8 5 μm 250 × 9.4 mm column) to yield, in relative order of elution, aspergillazine D/E (**11**/**12**; 5.1 mg, 0.76%), ferulic acid (**3**; 0.6 mg, 0.09%), aspergillazine C (**9**/**10**; 1.9 mg, 0.28%), aspergillazine B (**9**/**10**; 2.9 mg, 0.43%), penicillazine (**7**; 3.2 mg, 0.48%), *E*-2-decenedioic acid (**2**; 1.4 mg, 0.21%) and aspergillazine A (**8**) (2.9 mg, 0.43%). All yields are calculated relative to the dry weight of the combined 50% H_2O–MeOH eluants (671 mg) prior to HPLC. None of these metabolites exhibited any inhibitory activity against *B. subtilis*, *S. cerevisiae*, *C. albicans*, *H. contortus* or NS-1 cells *in vitro*.

Those fractions that did not display "penicillazine like" molecules were subjected to multiple HPLC fractionation with either gradient elution (4.2 mL min^{-1}, 70% H_2O–MeCN to 55% H_2O–MeCN over 12 min through a Zorbax SB-C_{18} 5 μm 250 × 9.4 mm column) or isocratic elution (3 mL min^{-1} of 50% H_2O–MeOH or 65% H_2O–MeOH through either Zorbax SB-C_8 5 μm 250 × 9.4 mm or Zorbax SB-phenyl, 5 μm 250 × 9.4 mm column) to yield 7*E*-,7′*E*-5,5′-diferulic acid (**4**; 2.0 mg, 0.30%), (7*E*-,7′*E*)-5,8′-diferulic acid (**5**; 1.2 mg, 0.18%) and riboflavin (**6**; 0.3 mg, 0.045%). All yields are calculated relative to the dry weight of the combined 50% H_2O–MeOH eluants (671 mg) prior to HPLC.

Viridicatumtoxin (1). Identified by ESI(±)MS, HRESI(+)-MS, UV, $[\alpha]_D$, ^{1}H and ^{13}C NMR, gHMBC and gHMQC comparison to literature data.[3,4]

***E*-2-Decenedioic acid (2).** Identified by ESI(±)MS and ^{1}H NMR comparison with literature data.[7]

Ferulic acid (3). Amorphous solid. Identified by ESI(±)MS and ^{1}H NMR comparison with a commercial authentic sample.

7*E*, 7′*E*-5,5′-Diferulic acid (4). Identified by ESI(±)MS and ^{1}H NMR comparison with literature data.[8,10,11]

7*E*, 7′*E*-8,5′-Diferulic acid (5). Identified by ESI(±)MS and ^{1}H NMR comparison with literature data.[8,10,11]

Riboflavin (6). Identified by ESI(±)MS and ^{1}H NMR comparison with a commercial authentic sample.

Penicillazine (trichodermamide A) (7). White solid. Identified by ESI(±)MS, HRESI(±)MS, UV, $[\alpha]_D$, ^{1}H and ^{13}C NMR, COSY, HMBC and HMQC comparison to literature data.[5,6]

Aspergillazine A (8). Yellow amorphous solid; $[\alpha]_D$ −103 (*c* 0.14, MeOH); UV (MeOH) λ_{max}/nm (ε/dm^3 mol^{-1} cm^{-1}) 205 (19 270), 245(sh), 337 (11 100) nm; ^{1}H NMR (CD_3OD, 400 MHz), see Table 1; ^{13}C NMR (CD_3OD, 100 MHz), see Table 1; ESI(+)MS (30 kV) *m*/*z* 471 (M + Na); HRESI(+)MS 471.0844 (M + Na, $C_{20}H_{20}N_2O_8SNa$ requires 471.0838).

Aspergillazine B (9). Yellow amorphous solid $[\alpha]_D$ −172 (*c* 0.07, MeOH); UV (MeOH) λ_{max}/nm (ε/dm^3 mol^{-1} cm^{-1}) 203 (17 850), 243(sh), 335 (9400) nm; ^{1}H NMR (CD_3OD, 500 MHz), see Table 2; ESI(+)MS (30 kV) *m*/*z* 473 (M + Na); HRESI(+)MS 473.0989 (M + Na, $C_{20}H_{22}N_2O_8SNa$ requires 473.0995).

Aspergillazine C (10). Yellow amorphous solid $[\alpha]_D$ +23 (*c* 0.08, MeOH); UV (MeOH) λ_{max}/nm (ε/dm^3 mol^{-1} cm^{-1}) 205 (16 400), 243(sh), 335 (7700) nm; ^{1}H NMR (CD_3OD, 500 MHz), see Table 2; ESI(+)MS (30 kV) *m*/*z* 473 (M + Na); HRESI(+)MS 473.0994 (M + Na, $C_{20}H_{22}N_2O_8SNa$ requires 473.0995).

Aspergillazine D/E (11/12). Yellow amorphous solid $[\alpha]_D$ −79 (*c* 0.14, MeOH); UV (MeOH) λ_{max}/nm (ε/dm^3 mol^{-1} cm^{-1}) 204 (17 280), 228(sh), 333 (11 400) nm; ^{1}H NMR (CD_3OD, 500 MHz), see Table 2; ESI(+)MS (30 kV) *m*/*z* 457 (M + Na); HRESI(+)MS 457.1230 (M + Na, $C_{20}H_{22}N_2O_9Na$ requires 457.1223).

Trichodermamide B (13). Re-fermentation of *A. unilateralis* (1 × ~30 g solid phase culture on wheat, 21 days, 28 °C) in the presence of 1% NaCl yielded an extract which, on analysis by C_8 LC/MS (1.0 mL min^{-1} 90% H_2O–MeCN to MeCN over 15 min through a C_8 Zorbax Eclipse XDB 5 μm 150 × 4.6 mm, extracted M + H ion chromatograms at *m*/*z* 451[^{35}Cl] and 453[^{37}Cl]) revealed low level production of an additional metabolite consistent with trichodermamide B (**13**).

Acknowledgements

We wish to thank Mrs Sally Duck (Monash University) and Dr Graham MacFarlane (University of Queensland) for providing HRMS data and Dr Ailsa Hocking, Food Science Australia, for fungal taxonomy. This research was sponsored in part by the Australian Research Council.

References

1 R. J. Capon, C. Skene, M. Stewart, J. Ford, R. A. J. O'Hair, L. Williams, E. Lacey, J. H. Gill, K. Heiland and T. Friedel, *Org. Biomol. Chem.*, 2003, **1**(11), 1856–1862.
2 M. Stewart, R. J. Capon, J. M. White, E. Lacey, S. Tennant, J. H. Gill and M. P. Shaddock, *J. Nat. Prod.*, 2004, **67**(4), 728–730.
3 R. D. Hutchison, P. S. Steyn and S. J. Van Rensburg, *Toxicol. Appl. Pharmacol.*, 1973, **24**(3), 507–509.
4 A. E. De Jesus, W. E. Hull, P. S. Steyn, F. R. Van Heerden and R. Vleggaar, *J. Chem. Soc., Chem. Commun.*, 1982, (16), 902–904.
5 Y. Lin, Z. Shao, G. Jiang, S. Zhou, J. Cai, L. L. P. Vrijmoed and E. B. G. Jones, *Tetrahedron*, 2000, **56**(49), 9607–9609.
6 E. Garo, C. M. Starks, P. R. Jensen, W. Fenical, E. Lobkovsky and J. Clardy, *J. Nat. Prod.*, 2003, **66**(3), 423–426.
7 O. C. H. Kwok, R. Plattner, D. Weisleder and D. T. Wicklow, *J. Chem. Ecol.*, 1992, **18**(2), 127–136.
8 J. Ralph, S. Quideau, J. H. Grabber and R. D. Hatfield, *J. Chem. Soc., Perkin Trans. 1*, 1994, (23), 3485–3498.
9 L. Panizzi, C. Caponi, S. Catalano, P. L. Cioni and I. Morelli, *J. Ethnopharmacol.*, 2002, **79**, 165–168.
10 R. D. Hartley and E. C. Jones, *Phytochemistry*, 1976, **15**, 1157–1160.
11 E. Larsen, M. F. Andreasen and L. P. Christensen, *J. Agric. Food. Chem.*, 2001, **49**, 3471–3475.
12 J. H. Gill, J. M. Redwin, J. A. van Wyk and E. Lacey, *Int. J. Parasitol.*, 1995, **25**, 463–470.